Spectroscopy of Tm and Ho in KYF_4 single crystals

2006 J. Phys.: Condens. Matter 18 2057

(http://iopscience.iop.org/0953-8984/18/6/018)

INSTITUTE OF PHYSICS PUBLISHING JOURNAL OF PHYSICS: CONDENSED MATTER

J. Phys.: Condens. Matter **18** (2006) 2057–2067 doi:10.1088/0953-8984/18/6/018

Spectroscopy of Tm and Ho in KYF_4 single crystals

Elisa Sani[1], **Alessandra Toncelli and Mauro Tonelli**

NEST—Dipartimento di Fisica, Università di Pisa, Largo Pontecorvo, 3-56127 Pisa, Italy

E-mail: sani@inoa.it

Received 30 September 2005, in final form 26 December 2005
Published 27 January 2006
Online at stacks.iop.org/JPhysCM/18/2057

Abstract

We report on the spectroscopic characterization of Tm:KYF_4 and Ho:KYF_4 single crystals. The energy level splittings are given, as well as the Judd–Ofelt parameters, the polarized absorption and emission cross sections and the energy transfer coefficients. This allows to have a deeper understanding of the Tm–Ho-codoped KYF_4 system and shows KYF_4 to be a promising material for widely tunable and efficient 2 μm laser operation.

1. Introduction

Interest in 2 μm eye-safe lasers has increased during recent years, as well as the number of their applications. 2 μm laser sources are potentially useful for a variety of atmospheric and space applications, including coherent Doppler velocimetry and gas detection [1], atmospheric wind sensors for full-scale earth observation satellites, and medical equipment. 2 μm lasers based on the thulium $^3F_4 \rightarrow {}^3H_6$ transition have been demonstrated [2] and also the holmium $^5I_7 \rightarrow {}^5I_8$ transition, which has a definitely higher lasing emission cross section and occurs at longer wavelengths [3], is of interest. Ho-codoping with Tm, to allow for diode pumping, has been investigated in a variety of crystalline materials. Efficient room-temperature laser emission at 2 μm based on the Ho $^5I_7 \rightarrow {}^5I_8$ transition has been reported in several Tm–Ho-codoped crystals [4]. Fluoride crystals, as compared with commonly used oxide matrices, have well known advantages in terms of active materials for laser applications, such as low phonon energy, which makes them particularly suitable for IR transitions. In addition, those of them which have noncubic structure are interesting because they are able to decrease the thermal lensing effect under strong pumping conditions. Widely tunable laser emission at room temperature in Tm–Ho-codoped KYF_4 (KYF) crystal has already been demonstrated [5]. In order to explain the Tm–Ho:KYF laser performances, in this work we focus on the characterization of Tm and Ho as single dopants in the KYF crystalline matrix.

2. Experimental details

Tm- and Ho-doped KYF single-crystalline samples were grown by means of the Czochralski method from oriented seeds using an automated home-made resistive furnace with a diameter

[1] Author to whom any correspondence should be addressed.

control system. To avoid any possible contamination of fluorides by hydroxile radicals, special care was devoted to the quality of the vacuum system, which has an ultimate pressure limit of a few 10^{-8} mbar. Crystal growth was carried out under 5N-purity argon atmosphere. The grown samples are 10% Tm-doped and 0.5% Ho-doped KYF. The growth powders (purified by AC Materials, Orlando, FLA) were handled in a glove box under 5N nitrogen flux to avoid any contamination by water or oxygen and were mixed in the suitable ratios, according to the non-congruent melting characteristics of the crystal [6]. The indicated RE^{3+} dopings (molar concentrations in the melt) were obtained by adding proper amounts of TmF_3 or HoF_3 to the $KF–YF_3$ powder mixture. For both the grown samples the growth rate was 0.5 mm h^{-1}, and the rotation rate was 10 RPM. The weight of the obtained boules was about 20 g. Typical dimensions were about 20 mm in diameter and 70 mm in length.

At first, the boules were analysed by the x-ray Laue technique. This allowed us to establish their monocrystalline character and crystallographic axis orientation. Then, the crystals were cut into small (a few mm^3) samples with an edge along the *c* crystallographic axis to investigate the polarization-dependent optical properties. Surfaces were optically polished using alumina powder.

Absorption polarized measurements at low and room temperature were performed by using a Cary 500 spectrophotometer. For diagnostic purposes, to check the presence of unwanted contaminants, we recorded the polarized absorption spectra of every sample from the UV to the IR wavelength region at room temperature. The resolution of these spectra was 0.6 nm up to 820 nm and 1.5 nm beyond that. The results allow us to infer that the samples are free of hydroxile or other unwanted contamination within the sensitivity of our instrument. The Stark level structure of Tm and Ho has been evaluated by means of 10 and 100 K polarized absorption measurements, keeping the samples on the cold finger of a closed-cycle He cryocooler.

In order to evaluate the emission cross section around 2 μm we recorded the polarized room-temperature emission spectra and we measured the room-temperature Ho $^5I_7$ lifetime. The Ho fluorescence spectra were acquired after 2.6 W excitation by a multiline argon laser (Coherent Innova 305 series). The signal was filtered by a germanium window and a Glan–Thompson polarizer, selected by the 300 g mm^{-1} grating of a 32 cm monochromator (Jobin Yvon TRIAX320) and detected by a cooled InSb detector. The resolution was 5.3 nm. The Ho $^5I_7$ lifetime was acquired by using a pulsed doubled Nd:YAG laser (Continuum Surelite I-10) at 532 nm as excitation source. The laser pulse energy was reduced to an undetectable value to minimize nonlinear power-dependent effects and to avoid the risk of crystal damage. The fluorescence decay signal, filtered by a germanium filter, was detected by the InSb photodiode, amplified by a fast device (response time about 1 μs) and sent to a digital oscilloscope.

In the case of the Tm-doped sample, the excitation source for stationary-state fluorescence measurements was a home-made tunable cw Ti:sapphire laser, tuned at 790 nm. The signal, after filtering by a silicon window ($\lambda_{cutoff} \simeq 1200$ nm), was selected by a 25 cm monochromator (Jobin Yvon HR250) equipped with a 300 g mm^{-1} grating and detected by a cooled InSb photodiode. The resolution was 3.6 nm. Both the Ho and Tm fluorescence spectra were corrected for the spectral response of the experimental apparatus using a black-body source at 3000 K. The experimental apparatus for the Tm $^3F_4$ lifetime measurement was the same as in the case of stationary fluorescence investigations, but for the excitation source which was a home-made pulsed tunable Ti:sapphire laser, tuned at 790 nm.

3. Spectroscopic analysis and laser parameters

All the crystals were investigated for their relative doping levels of both Tm and Ho ions by comparing the intensities of the room-temperature absorption bands. We found that the relative

Table 1. Experimental energy levels of Tm:KYF. $\Delta\mathcal{E}$ is the resolution of the measurement; $\mathcal{N}_{exp}$ and $\mathcal{N}_{theor}$ are the experimental and theoretical number of sublevels of the given multiplet.

Multiplet	Energy (cm^{-1})	$\Delta\mathcal{E}$ (cm^{-1})	$\mathcal{N}_{exp}$	$\mathcal{N}_{theor}$
$^3F_4$	5526 5548 5570 5579 5596 5624 5638 5657 5671 5765 5772 5800 5810 5848 5853 5965 5978 5991 6008 6040 6048 6051 6065 6072 6092 6104 6112 6114 6121	2	29	9
$^3H_5$	8255 8294 8317 8327 8342 8371 8426 8471 8529 8560 8593 8625 8647 8669 8695 8714 8891	3	17	11
$^3H_4$	12 552 12 578 12 602 12 637 12 678 12 693 12 710 12 788 12 832 12 854 12 886 12 901 12 933 12 951 12 968 12 987 13 017 13 035	5	18	9
$^3F_3 + {}^3F_2$	14 556 14 576 14 601 14 617 14 669 14 698 15 069 15 083 15 119 15 248 15 269 15 287 15 320 15 340 15 375 15 453	10	16	12
$^1G_4$	20 892 20 953 21 000 21 213 21 274 21 487 21 535 21 598 21 693	13	9	9
$^1D_2$	28 023 28 117 28 195	30	3	3
$^5I_6 + {}^3P_0$	34 346 34 510 34 880 35 038 35 338 35 574 35 663	50	7	14
$^3P_1$	36 540 36 670	55	2	3
$^3P_2$	38 270 38 461 38 670	65	3	5

doping ratios among the various samples inside the crystals were approximately the same as in the melt.

In order to give the energy positions of the Stark sublevels of Tm and Ho multiplets, we performed absorption measurements at low temperature on the 10% Tm-doped and the 0.5% Ho-doped samples. The polarized 10 K absorption spectra of Tm:KYF are shown in figure 1 and those of Ho:KYF are shown in figure 2. Assignments to $^{2S+1}L_J$ terms are given in tables 1 and 2. In the case of holmium, the small absorption connected to the low doping level of the sample together with the presence of a strong water absorption band superimposed to our $^5I_8 \rightarrow {}^5I_7$ transition did not allow us to acquire meaningful spectra relative to this holmium transition by our air-filled spectrophotometer. The low doping level is also responsible for the very poor signal-to-noise ratio in the case of the $^5I_5$ and $^5I_4$ absorption bands, which prevented a clear assignment of the energy level splitting of these multiplets. For these reasons, the holmium $^5I_7$, $^5I_5$ and $^5I_4$ absorption bands have not been reported in table 2 and in figure 2. In the absence of crystal-field calculations for both Tm:KYF and Ho:KYF, the experimental lines have been assigned in analogy with the results given in the literature for $LaCl_3$ [7] and $LiYF_4$ [8, 9]. In the case of Ho doping, our results agree with the literature data for KYF (the $^5I_6$ and $^5S_2 + {}^5F_4$ splittings are given in [10] and the $^5F_5$ splitting in [11]) within the resolution of our experimental data. To discriminate the absorption lines coming from higher sublevels of the ground state, all the polarized absorption bands have also been acquired at 100 K, and these 'hot lines' were identified by a comparison of the 10 and 100 K spectra. The 10 K peaks arising from excited sublevels of the ground state are not listed in tables 1 and 2.

As a comment to the 10 K absorption measurements, it is worth noticing that for some multiplets (e.g., the Tm manifolds from $^3F_4$ to $^3F_3 + {}^3F_2$) the experimental number of lines is larger than the theoretical one. This disagreement can be explained by the presence of many

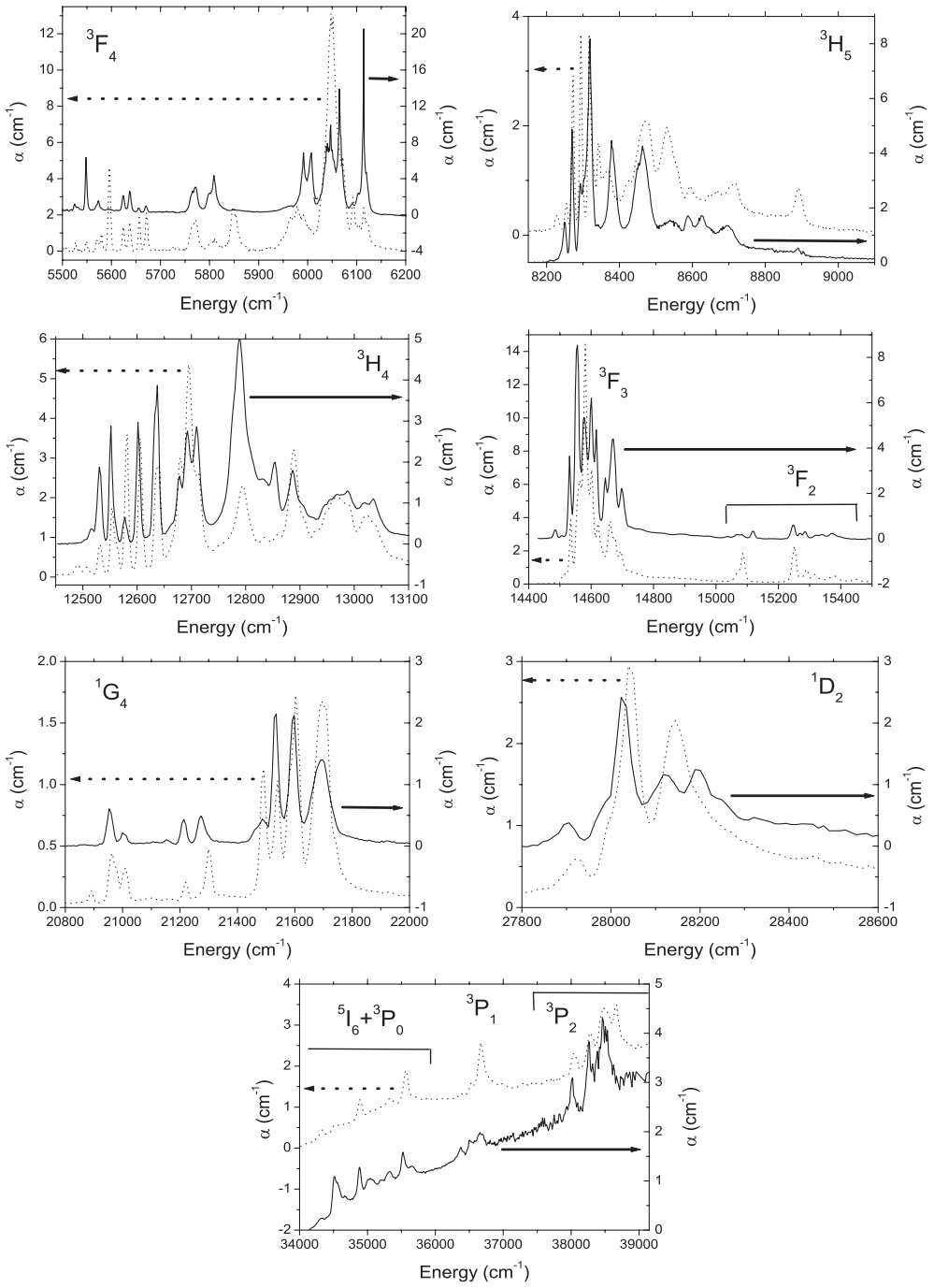

Figure 1. Polarized Tm:KYF absorption spectra at 10 K. The solid line refers to **E** ∥ **c** polarization, and the dotted line to **E** ⊥ **c**.

different crystallographic sites due to the disordered structure of the host. In contrast, in some cases (e.g., the high-lying levels of Tm and all the manifolds of Ho) the number of peaks is

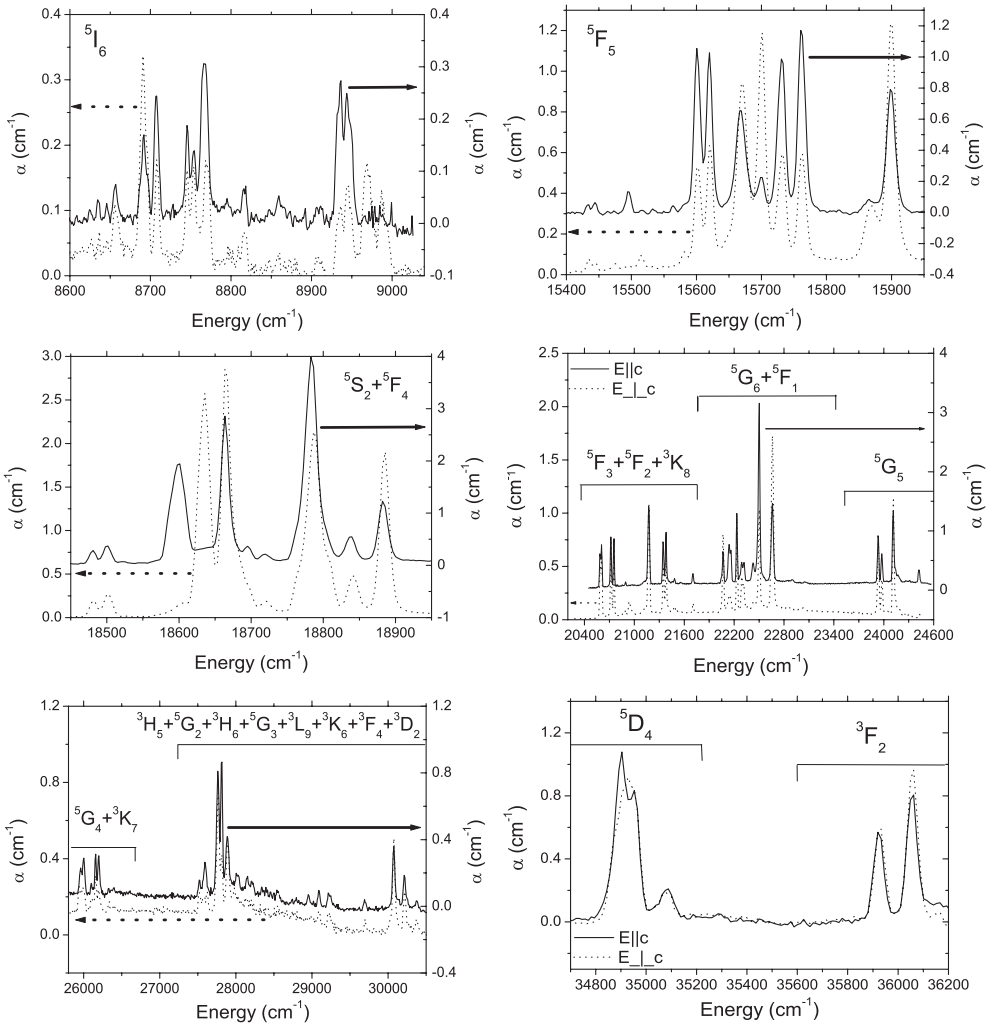

Figure 2. Polarized Ho:KYF absorption spectra at 10 K. The $^5I_5$ absorption band has not been included because of its poor signal-to-noise ratio. Solid line: $\mathbf{E} \parallel \mathbf{c}$ polarization. Dotted line: $\mathbf{E} \perp \mathbf{c}$.

smaller than the theoretical one. This can be explained, in case of Tm by the poor resolution arising from the signal-to-noise ratio, and in the case of Ho by the small absorption intensity due to the low doping level which produced non-optimal noise conditions. Moreover, the broadness of the absorption spectrum even at low temperature can be ascribed to the disordered characteristics of the crystal [12]. The broadness is increased at higher temperatures by thermal effects (figure 3). This peculiar width is appealing for different reasons: first, in absorption because it lifts the demands on the pump source wavelength control (which is particularly useful in the case of diode laser pumping) and second, in emission, when cw tunable or pulsed operation is concerned.

By means of the room-temperature polarized absorption spectra we carried out a Judd–Ofelt analysis on the samples [13, 14] in order to estimate the radiative lifetime of the energy levels involved in 2 μm emission and the Judd–Ofelt parameters Ω_j ($j = 2, 4, 6$). In our

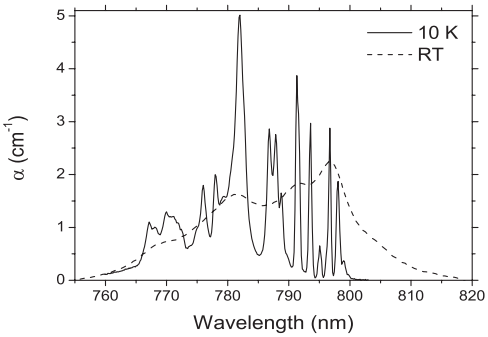

Figure 3. Comparison of the $\mathbf{E} \parallel \mathbf{c}$ $^3H_6 \rightarrow {}^3H_4$ absorption band at 10 K and room temperature (RT).

Table 2. Experimental energy levels of Ho:KYF. The meaning of the symbols is the same as in table 1.

Multiplet	Energy (cm^{-1})	$\Delta\mathcal{E}$ (cm^{-1})	$\mathcal{N}_{exp}$	$\mathcal{N}_{theor}$
$^5I_6$	8656 8691 8708 8745 8768 8936 8944 8969 8987	4	9	13
$^5F_5$	15 434 15 444 15 601 15 620 15 669 15 700 15 731 15 760 15 865 15 901	7	10	11
$^5S_2 + {}^5F_4$	18 600 18 636 18 664 18 695 18 783 18 804 18 837 18 882	10	8	14
$^5F_3 + {}^5F_2 + {}^3K_8$	20 585 20 606 20 894 20 938 21 124 21 173 21 345 21 381 21 482 21 706	15	10	29
$^5G_6 + {}^5F_1$	22 065 22 138 22 163 22 291 22 316 22 428 22 502 22 660	20	8	16
$^5G_5$	23 935 23 977 24 114 24 160 24 423	25	5	11
$^5G_4 + {}^3K_7$	25 960 26 001 26 100 26 157 26 198	25	5	24
$^3H_5 + {}^5G_2 + {}^3H_6$ $+ {}^5G_3 + {}^3L_9 + {}^3K_6$ $+ {}^3F_4 + {}^3D_2$	27 518 27 594 27 762 27 816 27 886 29 019 28 145 29 095 29 214 29 691 30 075 30 221 30 377	25	13	82
$^5D_4$	34 928 35 080	35	2	9
$^3F_2$	36 062	35	1	5

calculations, we considered the most important bands. Owing to the trigonal structure of the crystal, we averaged the data over the $\mathbf{E} \parallel \mathbf{c}$ and $\mathbf{E} \perp \mathbf{c}$ polarizations, as suggested in [15]. For the bands where the lines of some different transitions overlapped, we considered the mean wavelength [16], and for the refractive index we used the averaged value $n = 1.42$ [17]. The reduced matrix elements were taken from [4]. In tables 3 and 4, we report the experimental and calculated oscillator strengths: the agreement is fairly satisfying. The intensity parameters we found are listed in table 5, together with those of YLF and YAG for comparison. On the whole, the Ω_j parameters are smaller in KYF than in YLF (this is particularly evident in the case of Tm, as for Ω_2 and Ω_6) showing the low oscillator strengths and small crystal-field parameters of KYF [26]. The parameters for Tm:KYF are somewhat more similar to those of YAG than those of YLF. For Ho-doping, both KYF and YAG show the same $\Omega_4 > \Omega_6 > \Omega_2$ trend, but the KYF intensity parameter are smaller. The theoretical Tm $^3H_4$ and $^3F_4$ and Ho $^5I_7$ lifetimes are 1.5, 39 and 31 ms respectively, in fair agreement with the measured values (1.7 ms for Tm $^3H_4$ and 43 ms for $^3F_4$ at 10 K [19] and 21 ms for Ho$^5I_7$ [12]), within the intrinsic uncertainties

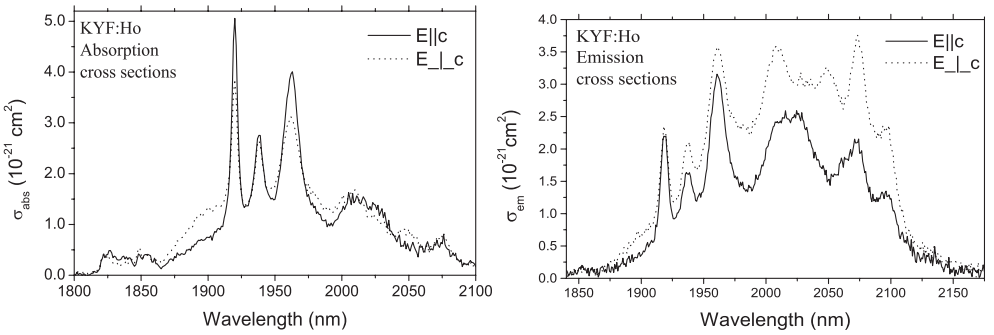

Figure 4. Polarized cross sections of the Ho $^5I_8$–$^5I_7$ transitions. Left: absorption ($^5I_8 \rightarrow {}^5I_7$). Right: emission ($^5I_7 \rightarrow {}^5I_8$).

Table 3. Experimental and calculated oscillator strengths of Tm:KYF.

Excited state	Barycentre (nm)	P_{exp} ($\times 10^{-7}$)	P_{calc} ($\times 10^{-7}$)
$^1D_2$	357	11.0	8.4
$^3F_3 + {}^3F_2$	685	15.6	16.8
$^3H_4$	786	10.1	10.7
$^3H_5$	1194	6.5	6.1
$^3F_4$	1710	4.1	3.9

Table 4. Experimental and calculated oscillator strengths of Ho:KYF.

Excited state	Barycentre (nm)	P_{exp} ($\times 10^{-7}$)	P_{calc} ($\times 10^{-7}$)
$^5F_1 + {}^5F_2 + {}^3K_8 + {}^5G_6 + {}^5F_1$	458	68.5	68.4
$^5S_2 + {}^5F_4$	536	30.4	20.7
$^5F_5$	624	17.3	20.8
$^5I_6$	1161	4.0	4.3
$^5I_7$	1966	4.5	6.2

Table 5. Comparison of the calculated Judd–Ofelt parameters Ω_j in KYF, $LiYF_4$ and YAG.

Crystal	Ω_2 (10^{-20} cm^2)	Ω_4 (10^{-20} cm^2)	Ω_6 (10^{-20} cm^2)	% RMS	Ref.
KYF:Tm	0.24	0.68	0.80	18	This work
$LiYF_4$:Tm	3.54	0.29	1.40	30	[18]
YAG:Tm	0.7	1.2	0.5		[4]
	0.89	1.08	0.68		[4]
	0.9	0.7	0.85		[4]
KYF:Ho	0.48	2.91	0.73	29	This work
$LiYF_4$:Ho	0.96	2.05	1.43	17	[18]
YAG:Ho	1.2	5.29	1.48		[4]

of the Judd–Ofelt approach. The lifetimes in KYF are much longer than in other crystals [3], confirming again the weak crystal-field parameters of the host [26].

In figure 4 (left) we report the absorption cross sections of the $^5I_7$ manifold of the holmium ion. The cross sections have been calculated from the absorption spectrum of the solely Ho-doped KYF, by dividing it by the holmium doping density in the crystal (5.2×10^{19} ions cm^{-3})

Table 6. Holmium emission cross sections in various hosts.

Host crystal	λ (nm)	σ_{em} (10^{-21} cm^2)	FWHM (nm)	Ref.
KYF **E** ∥ **c**	1962	3.1	185	This work
KYF **E** ⊥ **c**	2073	3.8	186	This work
$KCaF_3$	2085	2.8		[3]
LaF_3	2050	3.3		[3]
$LiYF_4$	2050	18.4	20	[3]
YAG	2098	9.8	40	[3]
$La_2Be_2O_5$	2088	4.2	50	[3]

assumed to be the same as in the melt. This assumption is justified both by the very low melt doping level and by observing that in KYF it is even possible to substitute Ho^{3+} for Y^{3+} completely without change in the crystal structure [20].

Emission cross sections have been calculated by the integral β–τ method [21], from the polarized emission spectra after correction for the spectral response of the system. The emission cross section σ_p for the emitted fluorescence in p-polarization is given by:

$$\sigma_p(\lambda) = \frac{\eta\lambda^5}{\frac{1}{3}\tau_{rad}\sum_s\left(\int \lambda I_s(\lambda)\,d\lambda\right)8\pi n^2 c} I_p(\lambda) \tag{1}$$

where λ is the wavelength, $I_j(\lambda)$ is the emission spectrum in j-polarization, τ_{rad} is the radiative lifetime of the emitting level, n is the refractive index, c is the speed of light and the summation is extended over all the possible polarizations. For the quantum efficiency value η we assumed unity.

In figure 4 (right) we show the room-temperature Ho $^5I_7 \rightarrow {}^5I_8$ emission cross sections. The polarized Ho spectra used in the calculations have been corrected for the spectral response of the experimental apparatus, as already indicated. The $^5I_7$ lifetime value we used is the one obtained from the measurements (22.1 ± 0.5 ms) because of the low doping level of the sample and it agrees with the literature value [22]. The Ho emission spectrum consists of a broad band with an FWHM of more than 180 nm. The peak values are about 3.5×10^{-21} cm^2 at 1962 nm and 3.8×10^{-21} cm^2 at 2073 nm in **E** ⊥ **c** polarization, and 3.1×10^{-21} cm^2 at 1961 nm in **E** ∥ **c** polarization. In table 6 the peak values of Ho emission cross sections in different hosts are compared. Even if the peak values of the 2 μm Ho emission cross sections in KYF are slightly lower than in other hosts [25], the advantage of KYF with respect to other crystals is the peculiar width of the emission cross section. This demonstrates the appealing perspectives of this material as an active medium for wide-tunability and/or pulsed solid-state lasers.

Thulium absorption cross sections (figure 5, left) have been calculated, like in the case of Ho-doping, assuming the Tm concentration in the crystal to be the same as in the melt. In fact also in the case of the Tm ion the isostructural $KTmF_4$ does exist [20]. Also, the Tm emission cross sections (figure 5, right) have been calculated by the integral β–τ method, from the corrected polarized emission spectra. As for the $^3F_4$ radiative lifetime, we used the value obtained from Judd–Ofelt calculations because our sample has a high doping level (10% mol) and therefore its measured lifetime cannot be considered as a reasonable approximation of the radiative one. In fact the value we measured at room temperature was 19.3 ± 0.3 ms, much shorter than the radiative one. The peak value of the Tm emission cross section is 0.9×10^{-21} cm^2 at 1917.2 nm in **E** ∥ **c** polarization and its FWHM is about 250 nm. This peak value is smaller than in other crystals (table 7), but its wide FWHM makes KYF a very interesting candidate to obtain tunable laser emission around 1.8–1.9 μm using thulium as the active ion.

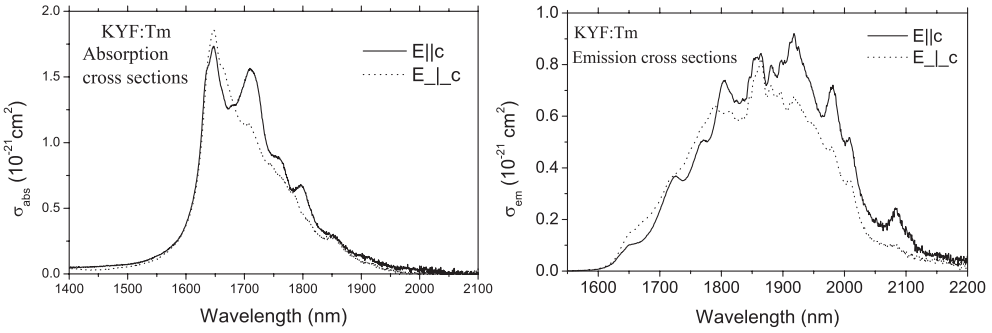

Figure 5. Polarized cross sections of the Tm $^3H_6$–$^3F_4$ transitions. Left: absorption ($^3H_6 \rightarrow {}^3F_4$). Right: emission ($^3F_4 \rightarrow {}^3H_6$).

Table 7. Thulium emission cross sections in various hosts.

Host crystal	λ (nm)	σ_{em} (10^{-21} cm^2)	FWHM (nm)	Ref.
KYF **E** ∥ **c**	1918	0.9	255	This work
KYF **E** ⊥ **c**	1864	0.8	250	This work
$KCaF_3$	1855	1.5		[3]
LaF_3	1850	2.5		[3]
$LiYF_4$	1902	3.3	3 peaks: ≃40	[3]
			1 peak: ≃20	[3]
YAG	2011	2.2		[3]
$La_2Be_2O_5$	1880	2.3	60	[3]

Other parameters that deeply affect the performance of a 2 μm Tm–Ho laser are the efficiencies of the energy transfer from the $^3F_4$ Tm level to the $^5I_7$ Ho level and of its back-transfer process. The values of these transfer coefficients can be easily evaluated from the emission and absorption cross sections shown in figures 4 and 5 by means of the Förster–Dexter theory [23]:

$$C_{\mathrm{Tm-Ho}} = \frac{9\chi^2 c}{16\pi^4 n^2} \int \sigma_{\mathrm{abs:Ho}} \sigma_{\mathrm{em:Tm}} \, \mathrm{d}\lambda \tag{2}$$

$$C_{\mathrm{Ho-Tm}} = \frac{9\chi^2 c}{16\pi^4 n^2} \int \sigma_{\mathrm{abs:Tm}} \sigma_{\mathrm{em:Ho}} \, \mathrm{d}\lambda \tag{3}$$

where χ^2 is a quantity that includes the orientational average and it is usually taken to be 2/3, c is the speed of light, n is the refractive index, and $\sigma_{\mathrm{abs:X}}$ and $\sigma_{\mathrm{em:X}}$ are the absorption and emission cross sections of X ion, respectively.

The values obtained for the Tm–Ho and Ho–Tm transfer coefficients are $C_{\mathrm{Tm-Ho}} = 4.8 \times 10^{-40}$ cm^6 s^{-1} and $C_{\mathrm{Ho-Tm}} = 6.3 \times 10^{-41}$ cm^6 s^{-1}. As expected, the back-transfer Ho $\rightarrow$ Tm coefficient is much smaller than that of the direct Tm $\rightarrow$ Ho energy transfer process. This is an important condition for an efficient Ho 2 μm laser. In table 8 the value of the Tm–Ho and Ho–Tm energy transfer coefficients in different hosts are compared. It should be noticed that KYF shows a value of the ratio between the direct-transfer and back-transfer coefficients higher than that of YLF and comparable to that of YAG. Therefore KYF seems promising for obtaining efficient laser emission under Tm–Ho codoping.

Table 8. Energy transfer coefficients in various hosts.

Host crystal	$C_{\mathrm{Tm–Ho}}$ (10^{-40} cm^6 s^{-1})	$C_{\mathrm{Ho–Tm}}$ (10^{-40} cm^6 s^{-1})	$C_{\mathrm{Tm–Ho}}/C_{\mathrm{Ho–Tm}}$	Ref.
KYF	4.8	0.6	$\simeq$ 8	This work
YAG	—	—	$\simeq$11.4	[24]
$LiYF_4$	17	2.7	6.3	[3]
$LiYF_4$		—	$\simeq$17.7	[24]

4. Conclusions

In this work two samples of Tm:KYF and Ho:KYF have been spectroscopically characterized at both low and room temperature. By means of 10 and 100 K absorption measurements, we assigned the absorption bands to $^{2S+1}L_J$ terms for both Tm and Ho ions in KYF and we gave their energy splittings. Using the room-temperature absorption spectra we carried out a Judd–Ofelt analysis, obtaining the intensity parameters Ω_j ($j = 2, 4, 6$) and the calculated radiative lifetime of Tm $^3F_4$ and $^3H_4$ and Ho $^5I_7$ multiplets. The obtained values turned out to be in agreement with the measured ones. By room-temperature emission spectroscopy we evaluated the emission cross sections for the Tm $^3F_4 \rightarrow {}^3H_6$ and Ho $^5I_7 \rightarrow {}^5I_8$ transitions. By means of the Förster–Dexter theory we calculated the $\mathrm{Tm}(^3F_4) \rightarrow \mathrm{Ho}(^5I_7)$ and the reverse $\mathrm{Ho}(^5I_7) \rightarrow \mathrm{Tm}(^3F_4)$ energy transfer coefficients, and we demonstrated the absence of a meaningful Ho-to-Tm back-transfer. The obtained results suggest KYF as a promising material for the development of tunable lasers emitting around 2 μm wavelength under Tm–Ho or Tm doping.

Acknowledgment

The authors wish to thank Ilaria Grassini for skill and competence in preparing the samples.

References

[1] Sudesh V and Piper J A 2000 Spectroscopy, modeling, and laser operation of thulium-doped crystals at 2.3 μm *IEEE J. Quantum Electron.* **36** 879–84
[2] Sudesh V and Goldys E M 2000 Spectroscopic properties of thulium-doped crystalline materials including a novel host, $La_2Be_2O_5$: a comparative study *J. Opt. Soc. Am.* B **17** 1068–76
[3] Payne S A, Chase L L, Smith L K, Kway W L and Krupke W F 1992 Infrared cross-section measurements for crystals doped with Er^{3+}, Tm^{3+}, and Ho^{3+} *IEEE J. Quantum Electron.* **28** 2619–30
[4] Kaminskii A A 1996 *Crystalline Lasers: Physical Processes and Operating Schemes* (Boca Raton, FL: CRC Press)
[5] Galzerano G, Sani E, Toncelli A, Della Valle G, Taccheo S, Tonelli M and Laporta P 2004 Widely tunable continuous-wave diode-pumped 2-μm Tm–Ho:KYF_4 laser *Opt. Lett.* **29** 715–7
[6] Chai B, Lefaucheur J, Pham A, Lutts G and Nicholls J 1993 Growth of high-quality single crystals of KYF_4 by TSSG method *Proc. SPIE* **1863** 131–5
[7] Dieke G H 1968 *Spectra and Energy Levels of Rare Earth Ions in Crystals* (New York: Interscience)
[8] Karayianis N, Wortman D E and Jenssen H P 1976 Analysis of the optical spectrum of Ho^{3+} in $LiYF_4$ *J. Phys. Chem. Solids* **37** 675–82
[9] Jenssen H P, Linz A, Leavitt R P, Morrison C A and Wortman D E 1975 Analysis of the optical spectrum of Tm^{3+} in $LiYF_4$ *Phys. Rev.* B **11** 92–101
[10] Peale R A, Weidner H, Summers P L, Zhang X X, Bass M and Chai B H T 1993 Comparative Fourier spectroscopy of Ho^{3+} and Yb^{3+} in KYF_4, BaY_2F_8 and $LiYF_4$ *OSA Proceedings on Advanced Solid-State Lasers* vol 15, ed A A Pinto and T Y Fan (Washington, DC: Optical Society of America) pp 450–3
[11] Peale R E, Weidner H, Summers P L and Chai B H T 1994 Site-selective spectroscopy of Ho^{3+}:KYF_4 *J. Appl. Phys.* **75** 502–6

[12] Sani E, Toncelli A, Tonelli M and Traverso F 2004 Growth and spectroscopic analysis of Tm, Ho:KYF_4 *J. Phys.: Condens. Matter* **16** 241–52
[13] Judd B R 1962 Optical absorption intensity of rare earth ions *Phys. Rev.* B **127** 750
[14] Ofelt G S 1962 Intensities of crystal spectra of rare earth ions *J. Chem. Phys.* **37** 511
[15] Merckle L D, Zandi B, Moncorgé R, Guyot Y, Verdun H R and McIntosh B 1996 Spectroscopy and laser operation of Pr, Mg:$SrAl_{12}O_{19}$ *J. Appl. Phys.* **79** 1849
[16] Weber M J, Varitimos T E and Matsinger B H 1973 Optical intensities of rare-earths ions in yttrium orthoaluminate *Phys. Rev.* B **8** 47
[17] Allik T A, Merckle L D, Utano R A, Chai B H T, Lefaucheur J L V, Voss H and Dixon G J 1993 Crystal growth, spectroscopy and laser performance of Nd^{3+}:KYF_4 *J. Opt. Soc. Am.* B **10** 633–7
[18] Li C, Guyot Y, Linares C, Moncorgé R and Joubert M F 1993 Radiative transition probabilities of trivalent rare-earth ions in $LiYF_4$ *OSA Proceedings on Advanced Solid-State Lasers* vol 15, ed A A Pinto and T Y Fan (Washington, DC: Optical Society of America) pp 91–5
[19] Sani E, Cornacchia F, Toncelli A and Tonelli M 2005 Spectroscopy and laser emission from Tm:KYF_4, in preparation
[20] Ardashnikova E I, Borzenkova M P and Novoselova A V 1980 Transformations in the series of potassium lanthanide double fluorides *Russ. J. Inorg. Chem.* **25** 833–6
[21] Aull B F and Jenssen H P 1982 Vibronic interactions in Nd:YAG resulting in nonreciprocity of absorption and stimulated emission cross sections *IEEE J. Quantum Electron.* **18** 925
[22] Möbert P E A, Diening A, Heumann E, Huber G and Chai B H T 1998 Room-temperature continuous-wave upconversion-pumped laser emission in Ho,Yb:KYF_4 at 756, 1070, and 1390 nm *Laser Phys.* **8** 210–3
[23] Dexter D L 1953 *J. Chem. Phys.* **21** 836
[24] Dinndorf K M and Jenssen H P 1994 Distribution of stored energy in the excited manifolds of Tm and Ho in 2 micron laser materials *OSA Proceedings on Advanced Solid-State Lasers* vol 20, ed T Y Fan and B H T Chai (Washington, DC: Optical Society of America) pp 131–5
[25] Sani E, Toncelli A, Tonelli M, Coluccelli N, Galzerano G and Laporta P 2005 Comparative analysis of Tm–Ho:KYF_4 laser crystals *Appl. Phys.* B **81** 847–51
[26] Zhang X X, Bass M, Chai B H T and Peale R E 1993 Comparison of Yb, Ho upconversion energy transfer in different fluoride crystals *OSA Proceedings on Advanced Solid-State Lasers* vol 15, ed A A Pinto and T Y Fan (Washington, DC: Optical Society of America) pp 253–7